Lanthanide Complexes of the Hexadentate N-Donor Podand Tris[3-(2-pyridyl)pyrazolyl]hydroborate: Solid-State and Solution Properties

Peter L. Jones, Angelo J. Amoroso, John C. Jeffery, Jon A. McCleverty,* Elefteria Psillakis, Leigh H. Rees, and Michael D. Ward*

School of Chemistry, University of Bristol, Cantock's Close, Bristol BS8 1TS, U.K.

Received May 28, 1996[⊗]

The hexadentate N_6-donor podand tris[3-(2-pyridyl)pyrazolyl]hydroborate (Tp^{Py}) contains 2-pyridyl fragments attached to the pyrazolyl C^3-positions such that each arm is a bidentate chelate. Three series of lanthanide(III) complexes were prepared: $[M(Tp^{Py})(MeOH)_2F][PF_6]$ (series **A**), $[M(Tp^{Py})(NO_3)_2]$ (series **B**), and $[M(Tp^{Py})_2][BPh_4]$ (series **C**). Crystallographic studies showed that series **A** and **B** have a 1:1 metal:Tp^{Py} ratio, with the metal ion lying within the podand cavity and the remaining coordination sites occupied by solvent molecules and/or counterions to give 9-coordination (**A**, with one fluoride and two methanol ligands) or 10-coordination (**B**, with two bidentate nitrate ligands). The **C** complexes were prepared in the absence of any coordinating anions and have a 1:2 metal:Tp^{Py} ratio with an unusual icosahedral geometry arising from coordination of the 12 nitrogen donors from two interleaved podands. Conductivity studies on the **B** complexes show that in water the nitrates dissociate to give $[M(Tp^{Py})(H_2O)_q](NO_3)_2$; the relaxivity of $[Gd(Tp^{Py})(NO_3)_2]$ in water is 4.4 s^{-1} mM^{-1}, a value comparable to those of clinically useful MRI contrast enhancement agents. Comparison of emission lifetimes of $[M(Tp^{Py})(NO_3)_2]$ (M = Eu, Tb) in H_2O/D_2O and CH_3OH/CD_3OD give values for q, the number of coordinated solvent molecules, of 3.6 (water) and 2.6 (methanol). The **C** complex $[Tb(Tp^{Py})_2][BPh_4]$ also has $q = 2.6$ in methanol, suggesting that partial ligand dissociation allows access of solvent molecules to the metal coordination sphere.

Introduction

The coordination chemistry of lanthanides has become of increasing significance in the last few years due to the wide variety of potential applications of lanthanide complexes. These applications include the use of luminescent [Eu(III), Tb(III)] complexes both in medicine as luminescent probes[1] and in the area of supramolecular photochemistry[2] and the use of highly paramagnetic complexes [generally of Gd(III)] as contrast agents to enhance the output from magnetic resonance imaging (MRI) scanners.[3]

Thermodynamically and kinetically stable lanthanide(III) complexes generally require high denticity ligands with hard donor sets such as nitrogen and anionic oxygen, as exemplified by the polyaminocarboxylates[4] and N-donor macrocyles with pendant carboxylate[5] or phosphonate groups.[6] We describe in this paper the preparation of the new hexadentate podand ligand tris[3-(2-pyridyl)pyrazolyl]hydroborate (Tp^{Py}) and the syntheses, crystal structures, and properties of some of its lanthanide complexes. These lanthanide complexes are of interest not only for their unusual structures and coordination environments (e.g., N_{12}-icosahedra) but also for their luminescence and NMR relaxivity properties, which make them of potential use as first-generation fluoroimmunoassay and MRI contrast agents.

The tris(pyrazolyl)borate family of ligands has been immensely popular with coordination chemists, due in part to the ease with which the ligands can be functionalized by attachment of substitutents to the C^3-positions of the pyrazolyl rings.[7] Substitutents in this position have generally been alkyl or aryl groups which, although themselves coordinatively innocent, can change the chemistry of the metal center by providing a sterically hindering and protective screen. This results in the kinetic stabilization of low coordination geometries and/or unusual ancillary ligands, and many such complexes are of particular interest in areas varying from metalloenzyme models[8] to new synthetic reagents.[9]

[⊗] Abstract published in *Advance ACS Abstracts,* December 15, 1996.

(1) (a) Soini, E.; Hemmila, I.; Dhalen, P. *Ann. Biol. Chem.* **1990**, *48*, 567. (b) Bünzli, J.-C. G. In *Lanthanide Probes in Life, Chemical and Earth Sciences, Theory and Practice;* Bünzli, J.-C. G., Choppin, G. R., Eds.; Elsevier: New York, 1989; pp 219−293. (c) Saha, A. K.; Kross, K.; Kloszewski, E. D.; Upson, D. A.; Toner, J. L.; Snow, R. A.; Black, C. D. V.; Desai, V. C. *J. Am. Chem. Soc.* **1993**, *115*, 11032. (d) Mukkala, V. M.; Heleniu, M.; Hemmila, I.; Kankare, J.; Takalo, H. *Helv. Chim. Acta* **1993**, *76*, 1361.

(2) (a) Sabbatini, N.; Guardigli, M.; Lehn, J.-M. *Coord. Chem. Rev.* **1993**, *123*, 201. (b) Piguet, C.; Bünzli, J.-C. G.; Bernardinelli, G.; Bochet, C. G.; Froidevaux, P. *J. Chem. Soc., Dalton Trans.* **1995**, 83. (c) Piguet, C.; Hopfgartner, G.; Williams, A. F.; Bünzli, J.-C. G. *J. Chem. Soc., Chem. Commun.* **1995**, 491.

(3) (a) Koenig, S. H.; Brown, R. D. *Prog. Nucl. Magn. Reson. Spectrosc.* **1990**, *22*, 487. (b) Lauffer, R. B. *Chem. Rev.* **1987**, *87*, 901. (c) Parker, D. *Chem. Br.* **1994**, 818. (d) Watson, A. D. *J. Alloys Compd.* **1994**, *207/208*, 14.

(4) (a) Pubanz, D.; González, G.; Powell, D. H.; Merbach, A. E. *Inorg. Chem.* **1995**, *34*, 4447. (b) Uggeri, F.; Aime, S.; Anelli, P. L.; Botta, M.; Brocchetta, M.; De Häen, C.; Ermondi, G.; Grandi, M.; Paoli, P. *Inorg. Chem.* **1995**, *34*, 633. (c) Paul-Roth, C.; Raymond, K. *Inorg. Chem.* **1995**, *34*, 1408.

(5) (a) Kim, W. D.; Keifer, G. E.; Maton, F.; McMillan, K.; Muller, R. N.; Sherry, A. D. *Inorg. Chem.* **1995**, *34*, 2233. (b) Inoue, M.; Navarro, R. E.; Inoue, M.; Fernando, Q. *Inorg. Chem.* **1995**, *34*, 6074. (c) Kumar, K.; Chang, C. A.; Francesconi, L. C.; Dischino, D. D.; Malley, M. F.; Gougoutas, J. Z.; Tweedle, M. F. *Inorg. Chem.* **1994**, *33*, 3567. (d) Aime, S.; Botta, M.; Crich, S. G.; Giovenzana, G. B.; Jommi, G.; Pagliarin, R.; Sisti, M. *J. Chem. Soc., Chem. Commun.* **1995**, 1885.

(6) (a) Aime, S.; Batsanov, A.; Botta, M.; Howard, J. A. K.; Parker, D.; Senanayake, K.; Williams, G. *Inorg. Chem.* **1994**, *33*, 4696. (b) Aime, S.; Botta, M.; Parker, D.; Williams, J. A. G. *J. Chem. Soc., Dalton Trans.* **1996**, 17.

(7) Trofimenko, S. *Chem. Rev.* **1993**, *93*, 943.

(8) Some representative recent examples: (a) Fujisawa, K.; Tanaka, M.; Morooka, Y.; Kitajima, N. *J. Am. Chem. Soc.* **1994**, *116*, 12079. (b) Fujisawa, K.; Morooka, Y.; Kitajima, N. *J. Chem. Soc., Chem. Commun.* **1994**, 623. (c) Qiu, D.; Kilpatrick, L.; Kitajima, N.; Spiro, T. G. *J. Am. Chem. Soc.* **1994**, *116*, 2585. (d) Ruf, M.; Weis, K.; Vahrenkamp, H. *J. Chem. Soc., Chem. Commun.* **1994**, 135. (e) Turowski, P. N.; Armstrong, W. H.; Liu, S.; Brown, S. N.; Lippard, S. J. *Inorg. Chem.* **1994**, *33*, 636. (f) Carrano, C. J.; Mohan, M.; Holmes, S. M.; de la Rosa, R.; Butler, A.; Charnock, J. M.; Garner, C. D. *Inorg. Chem.* **1994**, *33*, 646.

S0020-1669(96)00621-0 CCC: $14.00 © 1997 American Chemical Society

Despite the ease with which C^3-substituents can be attached to the tris(pyrazolyl)borate core, tris[3-(2-pyridyl)pyrazolyl]-hydroborate is the first example of a podand-type ligand prepared by attachment of additional coordinating groups (here, 2-pyridyl substituents).[10,11] Each arm of the ligand is thus an N,N-bidentate chelate. Other types of podand ligand, in which three (or more) chelating arms are linked by a bridgehead atom, are common and are used to impart high kinetic and thermodynamic stability to metal complexes. Well-known naturally occurring examples include the Fe(III)-binding siderophores;[12] synthetic tris-chelate podands have been prepared containing a wide variety of side arms based on chelating groups such as polypyridines,[13] catechol,[14] salicylaldimine,[15] 1,2-diaminoethane,[16] and the N,O-donor podands mentioned above which are tailored for coordination to lanthanides.

Parts of this work have been published as preliminary communications.[10]

Experimental Section

General Details. The following instruments were used for routine spectroscopic and electrochemical work: ^{1}H NMR spectroscopy; Jeol GX-270, Lambda-300 or GX-400 spectrometers; electron-impact (EI) and fast-atom bombardment (FAB) mass spectrometry, VG-Autospec; UV−visible spectrophotometry, Perkin-Elmer Lambda 2; FT-IR spectrometry, Perkin-Elmer 1600; conductivity measurements were performed with a Wayne Kerr B224 Universal Bridge at 298 K using 0.4 mmol of aqueous solutions, and the values quoted are corrected for the contribution of the solvent.

Luminescence spectra were recorded using a Perkin-Elmer LS-50B spectrofluorometer equipped with a Hamamatsu R928 photomultiplier tube, using excitation and emission slit widths of 5 nm. Phosphorescence lifetimes (τ) were measured with the instrument in time-resolved mode and are the average of at least three independent measurements which were made by monitoring the decay at a wavelength corresponding to the maximum intensity of the emission spectrum, following pulsed excitation. The intensity of the emission after the pulsed excitation was monitored after 20 different delay times spanning at least two lifetimes. The resulting first-order decay curves gave linear ln I vs t plots from which the lifetime was calculated by $\tau = \ln 2/\text{slope}$. The number of coordinated solvent molecules (q) for the Eu(III) and Tb(III) complexes was calculated from $q = n[\tau_H^{-1} - \tau_D^{-1}]$ where τ_H is the lifetime in the protonated solvent (H_2O or MeOH), τ_D is the lifetime in the corresponding deuterated solvent, and the values of n are 1.05 (Eu in water/D_2O), 4.2 (Tb in water/D_2O), 2.1 (Eu in CH_3OH/CD_3OD), or 8.4 (Tb in CH_3OH/CD_3OD).[2a,17]

NMR relaxivities were determined by monitoring the recovery of the proton signal of HOD (present in commercial D_2O) following pulsed excitation, after the method of ref 5b. Solution concentrations were 0.5 mM, and the relaxivity r_1 was determined from the equation $T_1^{-1} = r_1[M] + T_s^{-1}$, where T_1 is the relaxation time of the HOD signal in the presence of the paramagnetic complex, T_s is the relaxation time of the solvent, and [M] is the concentration of the paramagnetic complex. All relaxivity measurements were made at 20 °C and 250 MHz using a Jeol GX-270 spectrometer.

All reagents and starting materials were obtained from commercial sources (Aldrich, Lancaster, Avocado) and used as received. 3-(2-Pyridyl)pyrazole was prepared according to the literature method.[10a,18]

Preparation of K(Tp^{Py}). A mixture of 3-(2-pyridyl)-pyrazole (5.8 g, 40 mmol) and KBH_4 (0.54 g, 10 mmol) was heated to 200 °C for 1 h. The melt was then cooled, excess **2** was dissolved in toluene, and the remaining white solid was collected and dried. Yield: 80%. IR: ν_{B-H} (KBr disk) = 2444 cm^{-1}. EI MS: m/z 444 ([Tp^{Py}]$^-$). ^{1}H NMR (acetone-d_6), d 8.54 (1 H, ddd, J = 4.8, 1.8, 1.0 Hz, pyridyl H^6), 7.7−7.8 (3 H, m, pyridyl H^3/H^5 and pyrazolyl[H^4 or H^5]), 7.15 (1 H, ddd, J = 7.3, 4.8, 1.5 Hz, pyridyl H^4), 6.66 (1 H, d, J = 2.2 Hz, pyrazolyl H^5 or H^4).

Preparations of Complexes. A. [M(Tp^{Py})(MeOH)$_2$F][PF$_6$] (Series A; M = Sm, Eu, Gd, Tb, Ho, Yb). A mixture of KTp^{py} (1 mmol) and $MCl_3 \cdot xH_2O$ (1 mmol) in methanol was stirred for 1 h, after which time a solution of NH_4PF_6 in water was added. On stirring for a further 30 min and cooling, a precipitate appeared which was collected by filtration, washed with water, and dried to give the products in 30−50% yield. [Eu(Tp^{Py})(MeOH)$_2$F][PF$_6$] was recrystallized by diffusion of ether vapor into a solution of the complex in MeCN/MeOH (1:1) to give X-ray quality colorless blocks.

B. [M(Tp^{Py})(NO$_3$)$_2$] (Series B; M = La, Pr, Sm, Eu, Gd, Tb, Er). To a solution of KTp^{Py} (1 mmol) in methanol (20 cm^3) was added a solution of the appropriate lanthanide(III) nitrate hydrate (1 mmol) in methanol (20 cm^3). The mixture was stirred for 30 min. During this time a white precipitate formed which was collected by filtration, washed with methanol, and dried. The yields were in the range 40−80%. The Pr, Eu, and Er complexes were recrystallized by diffusion of ether into concentrated dmf solutions to give X-ray quality crystals. ^{1}H NMR spectrum of the diamagnetic complex [La(Tp^{Py})(NO$_3$)$_2$] (270 MHz, CD_3OD): δ 8.84 (1H, br s, pyridyl H^6), 7.98 (3H, m, pyridyl H^3, H^5 and one pyrazolyl H), 7.50 (1H, t, J = 5.6 Hz, pyridyl H^4), 6.87 (1H, d, J = 2.4 Hz, pyrazolyl H).

C. [M(Tp^{Py})$_2$][BPh$_4$] (Series C; M = La, Sm, Eu, Gd, Tb). A mixture of KTp^{py} (1 mmol) and the appropriate lanthanide(III) chloride hydrate (0.5 mmol) in MeOH (20 cm^3) was stirred for 10 min, after which time a methanolic solution containing excess $NaBPh_4$ was added. Concentration *in vacuo* produced an off-white precipitate which was collected by filtration, washed copiously with water, and dried. The solids were then dissolved in MeCN and filtered to remove any $KBPh_4$ that may have precipitated, before recrystallization from MeCN/Et_2O by vapor diffusion. The yields were in all cases 90−100%. ^{1}H NMR spectrum of the diamagnetic complex [M(Tp^{Py})$_2$][BPh$_4$] (300 MHz, acetone-d_6): δ 8.26 (1H, d, J = 2.4 Hz, pyrazolyl H), 7.18 (2H, m, pyridyl H^4, H^6), 6.74 (1H, d, J = 2.4 Hz, pyrazolyl H), 6.40 (1H, m, pyridyl H^5), 6.22 (1H, d, J = 5.0 Hz, pyridyl H^3). Protons from [BPh$_4$]$^-$ are also apparent at 7.34, 6.92, and 6.79 ppm (relative integrals 2:2:1).

Characterization data for all of the complexes are in Table 1.

(9) (a) Gorrell, I. B.; Looney, A.; Parkin, G. *J. Chem. Soc., Chem. Commun.* **1990**, 220. (b) Han, R.; Gorrell, I. B.; Looney, A. G.; Parkin, G. *J. Chem. Soc., Chem. Commun.* **1991**, 717.
(10) (a) Amoroso, A. J.; Cargill Thompson, A. M. W.; Jeffery, J. C.; Jones, P. L.; McCleverty, J. A.; Ward, M. D. *J. Chem. Soc., Chem. Commun.* **1994**, 2751. (b) Amoroso, A. J.; Jeffery, J. C.; Jones, P. L.; McCleverty, J. A.; Rees, L.; Rheingold, A. L.; Sun, Y.; Takats, J.; Trofimenko, S.; Ward, M. D.; Yap, G. P. A. *J. Chem. Soc., Chem. Commun.* **1995**, 1881.
(11) (a) Amoroso, A. J.; Jeffery, J. C.; Jones, P. L.; McCleverty, J. A.; Ward, M. D. *Polyhedron* **1996**, *15*, 2023. (b) Bardwell, D. A.; Jeffery, J. C.; Jones, P. L.; McCleverty, J. A.; Ward, M. D. *J. Chem. Soc., Dalton Trans.* **1995**, 2921. (c) Amoroso, A. J.; Jeffery, J. C.; Jones, P. L.; McCleverty, J. A.; Thornton, P.; Ward, M. D. *Angew. Chem., Int. Ed. Engl.* **1995**, *34*, 1443.
(12) Miller, M. J. *Chem. Rev.* **1989**, *89*, 1563.
(13) (a) Ziessel, R.; Lehn, J.-M. *Helv. Chim. Acta* **1990**, *73*, 1149. (b) De Cola, L.; Barigelletti, F.; Balzani, V.; Belser, P.; von Zelewsky, A.; Vögtle, F.; Ebmayer, F.; Grammenudi, S. *J. Am. Chem. Soc.* **1988**, *110*, 7210. (c) Belser, P.; von Zelewsky, A.; Frank, M.; Seel, C.; Vögtle, F.; De Cola, L.; Barigelletti, F.; Balzani, V. *J. Am. Chem. Soc.* **1993**, *115*, 4076. (d) Leize, A.; Van Dorsselaer, R.; Krämer, R.; Lehm, J.-M. *J. Chem. Soc., Chem. Commun.* **1993**, 990. (e) Sheldon, P.; Errington, W.; Moore, P.; Rawle, S. C.; Smith, S. M. *J. Chem. Soc., Chem. Commun.* **1994**, 2489.
(14) (a) Hahn, F. E.; Rupprecht, S.; Moock, K. H. *J. Chem. Soc., Chem. Commun.* **1991**, 224. (b) Butler, A.; de la Rosa, R.; Zhou, Q.; Jhanji, A.; Carrano, C. J. *Inorg. Chem.* **1992**, *31*, 5072. (c) Karpishin, T. B.; Stack, T. D. P.; Raymond, K. N. *J. Am. Chem. Soc.* **1993**, *115*, 6115. (d) Tse, B.; Kishi, Y. *J. Am. Chem. Soc.* **1993**, *115*, 7892. (e) Aguiari, A. Bullita, E.; Casellato, U.; Guerriero, P.; Tamburini, S.; Vigato, P. I.; Russo, U. *Inorg. Chim. Acta* **1994**, 219, 135.
(15) (a) Ramesh, K.; Mukherjee, R. *J. Chem. Soc., Dalton Trans.* **1991**, 3259. (b) Liu, S.; Wong, E.; Rettig, S. J.; Orvig, C. *Inorg. Chem.* **1993**, *32*, 4268. (c) Chandra, S. K.; Chakravorty, P.; Chakravorty, A. *J. Chem. Soc., Dalton Trans.* **1993**, 863.
(16) (a) McAuley, A.; Subramanian, S.; Whitcombe, T. W. *J. Chem. Soc., Dalton Trans.* **1993**, 2209. (b) Perkovic, M. E.; Hegg, M. J.; Endicott, J. F. *Inorg. Chem.* **1991**, *30*, 3140.
(17) Horrocks, W. D.; Sudnick, D. R. *Acc. Chem. Res.* **1981**, *14*, 384.
(18) (a) Brunner, H.; Scheck, T. *Chem. Ber.* **1992**, *125*, 701. (b) Lin, Y.; Lang, S. A. *J. Heterocycl. Chem.* **1977**, *14*, 345.

Table 1. Characterization Data for the New Complexes

complex	FAB mass spectral data,[a] *m/z*	ν(B−H), cm^{-1}	elemental analyses[b] % C	% H	% N	complex	FAB mass spectral data,[a] *m/z*	ν(B−H), cm^{-1}	elemental analyses[b] % C	% H	% N
[Sm(Tp^{Py})(MeOH)$_2$F][PF$_6$]	757 {Sm(Tp^{Py})F(PF$_6$)}, 613 {Sm(Tp^{Py})F}	2479	*c*			[Eu(Tp^{Py})(NO$_3$)$_2$]	659 {Eu(Tp^{Py})(NO$_3$)}, 597 {Eu(Tp^{Py})}	2484	*c*		
[Eu(Tp^{Py})(MeOH)$_2$F][PF$_6$]	761 {Eu(Tp^{Py})F(PF$_6$)}, 616 {Eu(Tp^{Py})F}	2491	*c*			[Gd(Tp^{Py})(NO$_3$)$_2$]	662 {Gd(Tp^{Py})(NO$_3$)}	2473	39.4 (39.7)	2.8 (2.6)	20.8 (21.2)
[Gd(Tp^{Py})(MeOH)$_2$F][PF$_6$]	768 {Gd(Tp^{Py})F(PF$_6$)}, 620 {Gd(Tp^{Py})F}	2489	*c*			[Tb(Tp^{Py})(NO$_3$)$_2$]	665 {Tb(Tp^{Py})(NO$_3$)}	2490	40.0 (39.6)	3.0 (2.6)	21.1 (21.2)
[Tb(Tp^{Py})(MeOH)$_2$F][PF$_6$]	767 {Tb(Tp^{Py})F(PF$_6$)}, 622 {Gd(Tp^{Py})F}	2482	*c*			[Er(Tp^{Py})(NO$_3$)$_2$]	672 {Er(Tp^{Py})(NO$_3$)}	2487	39.8 (39.2)	2.6 (2.6)	20.8 (21.0)
[Ho(Tp^{Py})(MeOH)$_2$F][PF$_6$]	775 {Ho(Tp^{Py})F(PF$_6$)}, 628 {Ho(Tp^{Py})F}	2485	*c*			[La(Tp^{Py})$_2$][BPh$_4$]	1028 {La(Tp^{Py})$_2$}	2493, 2450	64.3 (64.2)	4.4 (4.3)	18.7 (18.7)
[Yb(Tp^{Py})(MeOH)$_2$F][PF$_6$]	784 {Yb(Tp^{Py})F(PF$_6$)}, 637 {Yb(Tp^{Py})F}	2489	*c*			[Sm(Tp^{Py})$_2$][BPh$_4$]	1040 {Sm(Tp^{Py})$_2$}	2484, 2455	*c*		
[La(Tp^{Py})(NO$_3$)$_2$]	645 {La(Tp^{Py})(NO$_3$)}	2484	*c*			[Eu(Tp^{Py})$_2$][BPh$_4$]	1041 {Eu(Tp^{Py})$_2$}, 597 {Eu(Tp^{Py})}	2480, 2451	63.6 (63.6)	4.6 (4.3)	18.8 (18.5)
[Pr(Tp^{Py})(NO$_3$)$_2$]	740 {Pr(Tp^{Py})+matrix}[d]	2483	*c*			[Gd(Tp^{Py})$_2$][BPh$_4$]	1045 {Gd(Tp^{Py})$_2$}	2480, 2452	*c*		
[Sm(Tp^{Py})(NO$_3$)$_2$]	656 {Sm(Tp^{Py})(NO$_3$)}, 596 {Sm(Tp^{Py})}	2473	40.0 (40.1)	2.7 (2.7)	21.2 (21.4)	[Tb(Tp^{Py})$_2$][BPh$_4$]	1048 {Tb(Tp^{Py})$_2$}	2482, 2452	*c*		

[a] The values quoted are those of the most intense component of the peak cluster. Due to the presence of broad peak envelopes (arising from a large number of isotopes) in some cases, and possible protonation by the matrix, these values may differ by one or two mass units from the the expected values. [b] Calculated values in parentheses. [c] Consistent analytical data could not be obtained despite several attempts (see text). [d] Matrix is 3-nitrobenzyl alcohol (mass 153).

Table 2. Crystallographic Data for the Six Crystal Structures

	{[Eu(Tp^{Py})F(MeOH)$_2$][PF$_6$]}$_{1.5}$·MeOH·Et$_2$O·(H$_2$O)$_2$	[Pr(Tp^{Py})(NO$_3$)$_2$]·(Et$_2$O)$_2$	[Eu(Tp^{Py})(NO$_3$)$_2$]·(dmf)·(Et$_2$O)$_{0.5}$	[Er(Tp^{Py})(NO$_3$)$_2$]·(dmf)·(Et$_2$O)$_{0.5}$	[Sm(Tp^{Py})$_2$][BPh$_4$]·Et$_2$O	[Eu(Tp^{Py})$_2$][BPh$_4$]·Et$_2$O
Formula	$C_{44}H_{58.5}N_{13.5}B_{1.5}Eu_{1.5}F_{10.5}O_7P_{1.5}$	$C_{32}H_{39}BN_{11}O_8Pr$	$C_{29}H_{31}BEuN_{12}O_{7.5}$	$C_{29}H_{31}BErN_{12}O_{7.5}$	$C_{76}H_{68}B_3N_{18}OSm$	$C_{76}H_{68}B_3EuN_{18}O$
fw	1378.6	857.5	830.4	845.7	1432.3	1433.9
cryst dimens	0.65 × 0.4 × 0.35	0.4 × 0.4 × 0.2	0.4 × 0.4 × 0.3	0.5 × 0.4 × 0.35	0.4 × 0.5 × 0.5	0.65 × 0.4 × 0.15
cryst syst	orthorhombic	triclinic	triclinic	triclinic	monoclinic	monoclinic
space group	*Pbnm*	$P\bar{1}$	$P\bar{1}$	$P\bar{1}$	$P2_1/c$	$P2_1/c$
a, Å	13.175(7)	10.616(3)	10.417(3)	10.478(2)	12.254(2)	12.159(3)
b, Å	19.544(11)	13.606(3)	13.381(4)	13.386(3)	24.847(4)	24.769(4)
c, Å	43.41(3)	14.670(4)	14.483(5)	14.435(2)	22.718(4)	22.685(5)
α, deg	90	113.66(2)	112.94(1)	112.92(1)	90	90
β, deg	90	94.08(2)	95.59(1)	94.83(1)	97.90(1)	97.94(1)
γ, deg	90	105.97(2)	105.29(1)	104.69(1)	90	90
V, Å^3	11177(11)	1826(1)	1747.3(9)	1766(1)	6851(2)	6766(1)
Z	8	2	2	2	4	4
D_{calc}, g cm^{-3}	1.639	1.560	1.578	1.591	1.389	1.408
μ(Mo Kα), mm^{-1}	1.811	1.399	1.859	2.440	0.918	0.989
F(000)	5536	872	834	844	2940	2944
diffractometer[a]	Siemens R3m/V	Siemens SMART	Siemens SMART	Siemens SMART	Siemens R3m/V	Siemens SMART
temp, K	293	293	173	293	293	293
2θ range, deg	5−45	3−46.5	4−50	3−46.5	5−40	4−50
no. of reflcns (collected/independent/R_{int})	7432/7432/0	7252/5103/0.029	8547/5999/0.022	6928/4919/0.026	6957/6331/0.016	31248/11848/0.037
no. of params refined	748	420	467	473	895	897
R_1, wR_2[b]	0.065, 0.188	0.041, 0.106	0.028, 0.078	0.027, 0.076	0.037, 0.107	0.040, 0.108
largest diff peak/hole, e Å^{-3}	1.859, −1.248	1.216, −0.504	1.127, −1.278	0.624, −0.788	0.355, −0.628	0.826, −0.581
a, *b* for weighting scheme[b]	0.0775, 72.75	0.0424, 4.36	0.0386, 3.93	0.0416, 2.16	0.0505, 17.60	0.0251, 16.86

[a] R3m/V: four-circle diffractometer with point detector. SMART: three-circle diffractometer with area detector. [b] Structure was refined on F_o^2 using all data: w$R_2 = [\sum[w(F_o^2 - F_c^2)^2]/\sum w(F_o^2)^2]^{1/2}$, where $w^{-1} = [\sigma^2(F_o^2) + (aP)^2 + bP]$ and $P = [\max(F_o^2,0) + 2F_c^2]/3$. The value in parentheses for R_1 is given for comparison with older refinements based on F_o with a typical threshold of $F \geq 4\sigma(F)$ and $R_1 = \sum||F_o| - |F_c||/\sum|F_o|$ and $w^{-1} = [\sigma^2(F_o) + gF_o^2]$.

Table 3. Selected Bond Lengths (Å) and Angles (deg) for $[Eu(Tp^{Py})F(MeOH)_2][PF_6]$

Eu(1)−F(173)	2.193(7)	Eu(2)−F(273)	2.197(8)
Eu(1)−O(171)	2.466(9)	Eu(2)−O(271)	2.549(8)
Eu(1)−O(172)	2.509(9)	Eu(2)−O(271a)	2.549(8)
Eu(1)−N(131)	2.529(10)	Eu(2)−N(231)	2.492(14)
Eu(1)−N(111)	2.533(11)	Eu(2)−N(211)	2.549(10)
Eu(1)−N(151)	2.551(10)	Eu(2)−N(211a)	2.549(10)
Eu(1)−N(121)	2.648(11)	Eu(2)−N(221)	2.659(10)
Eu(1)−N(141)	2.659(11)	Eu(2)−N(241)	2.660(10)
Eu(1)−N(161)	2.690(10)	Eu(2)−N(221a)	2.659(10)
N(111)−Eu(1)−N(131)	72.7(3)	N(211)−Eu(2)−N(231)	71.9(4)
N(131)−Eu(1)−N(151)	70.8(3)	N(231)−Eu(2)−N(211a)	71.9(4)
N(111)−Eu(1)−N(151)	65.2(3)	N(211)−Eu(2)−N(211a)	65.4(5)
N(111)−Eu(1)−N(121)	61.6(3)	N(211)−Eu(2)−N(221)	61.5(3)
N(131)−Eu(1)−N(141)	61.5(3)	N(231)−Eu(2)−N(241)	62.6(5)
N(151)−Eu(1)−N(161)	61.8(3)	N(211a)−Eu(2)−N(221a)	61.5(3)
N(141)−Eu(1)−O(171)	70.3(3)	N(241)−Eu(2)−O(271)	69.2(2)
O(171)−Eu(1)−N(121)	69.5(3)	O(271)−Eu(2)−N(221)	68.0(3)
N(121)−Eu(1)−N(161)	79.6(3)	N(221)−Eu(2)−N(221a)	79.3(4)
N(161)−Eu(1)−O(172)	67.3(3)	N(221a)−Eu(2)−O(271a)	68.0(3)
O(172)−Eu(1)−N(141)	66.8(3)	O(271a)−Eu(2)−N(241)	69.2(2)
N(121)−Eu(1)−F(173)	77.6(3)	N(221)−Eu(2)−F(273)	77.0(3)
N(141)−Eu(1)−F(173)	78.1(3)	N(241)−Eu(2)−F(273)	77.9(4)
N(161)−Eu(1)−F(173)	77.6(3)	N(221a)−Eu(2)−F(273)	77.0(3)
N(112)−B(1)−N(132)	111.0(11)	N(212)−B(2)−N(232)	110.8(11)
N(112)−B(1)−N(152)	105.6(11)	N(212)−B(2)−N(212a)	106(2)
N(132)−B(1)−N(152)	108.9(11)	N(232)−B(2)−N(212a)	110.8(11)

Table 4. Selected Bond Lengths (Å) and Angles (deg) for $[M(Tp^{Py})(NO_3)_2]$ (M = Pr, Eu, Er)

	Pr	Eu	Er
M−O(2)	2.558(4)	2.494(3)	2.457(3)
M−O(3)	2.606(4)	2.563(2)	2.486(3)
M−O(5)	2.604(4)	2.528(3)	2.427(3)
M−O(6)	2.586(4)	2.537(2)	2.527(3)
M−N(12)	2.547(4)	2.489(3)	2.428(3)
M−N(32)	2.584(5)	2.526(3)	2.478(3)
M−N(52)	2.585(4)	2.533(3)	2.476(3)
M−N(21)	2.738(4)	2.692(3)	2.671(3)
M−N(41)	2.746(5)	2.698(3)	2.637(4)
M−N(61)	2.719(5)	2.679(3)	2.678(3)

	Pr	Eu	Er
N(12)−M−N(32)	71.7(2)	72.08(9)	74.52(12)
N(12)−M−N(52)	72.12(14)	73.07(10)	73.70(12)
N(32)−M−N(52)	63.3(2)	64.14(9)	64.86(12)
N(12)−M−N(21)	61.22(14)	62.57(9)	63.03(11)
N(32)−M−N(41)	60.57(14)	61.68(9)	62.94(11)
N(52)−M−N(61)	61.08(14)	62.37(9)	62.25(11)
N(21)−M−O(2)	68.84(14)	68.86(8)	70.96(11)
O(2)−M−N(61)	70.93(14)	72.71(9)	69.20(11)
N(61)−M−N(41)	77.4(2)	75.25(9)	73.84(11)
N(41)−M−O(5)	67.80(14)	68.35(9)	72.41(11)
O(5)−M−N(21)	71.67(14)	71.18(8)	69.74(10)
O(2)−M−O(3)	49.54(13)	50.60(8)	51.41(11)
O(5)−M−O(6)	49.30(14)	50.56(8)	51.57(10)
N(11)−B−N(31)	110.8(5)	109.8(3)	109.2(4)
N(11)−B−N(51)	109.2(5)	109.3(3)	109.4(4)
N(31)−B−N(51)	106.9(5)	105.5(3)	105.6(4)

X-ray Crystal Structure Determinations. To prevent loss of solvent from the crystals, suitable crystals were either mounted in thin-walled glass capillary tubes containing some of the mother liquor or quickly transferred from the mother liquor to a stream of cold N_2 at −100 °C on the diffractometer. Table 2 contains the details of the crystal parameters, data collection, and refinement. In all cases the structures were solved by conventional heavy-atom or direct methods and refined by the full-matrix least-squares method on all F^2 data using the SHELXTL 5.03 package on Silicon Graphics Indigo-R4000 or Indy computers.[19] In all cases, non-hydrogen atoms were refined with anisotropic thermal parameters; hydrogen atoms were included in calculated positions and refined with isotropic thermal parameters which were ∼1.2 (aromatic CH) or 1.5 times (Me) the equivalent isotropic thermal parameters of their parent carbon atoms.

For those crystals examined using the R3m/v four-circle diffractometer (graphite-monochromatized Mo Kα radiation, $\bar{\lambda} = 0.710\ 73$ Å), a unique set of data was collected by using the Wyckoff ω-scan method with variable scan speeds according to the intensity of the reflection. Check reflections (3 for every 97 reflections collected) were used to provide a correction for any crystal decay during the data collection. The data were corrected for Lorentz and polarization effects, and for absorption effects by an empirical method using azimuthal scan data.

For the remaining crystals, examined using the Siemens SMART CCD area detector three-circle diffractometer (Mo *K*α radiation, graphite monochromator, $\bar{\lambda} = 0.710\ 73$ Å), the following method was used. For three settings of ϕ, narrow data "frames" were collected for 0.3° increments in ω. Approximately a full hemisphere of data was collected for each complex. At the end of data collection, the first 50 frames of data were recollected to establish that crystal decay had not taken place during the course of data collection. The substantial redundancy in data allows empirical absorption corrections to be applied using multiple measurements of equivalent reflections. Data frames were collected for 10−30 s/frame, depending on the intensity of the data, giving an overall time for data collection of 7−18 h. The data frames were integrated using SAINT and were merged to give a unique data set during structure solution and refinement with SHELXL.[19]

$[Eu(Tp^{Py})F(MeOH)_2][PF_6]$ crystallizes as $[Eu(Tp^{Py})F(MeOH)_2]_{1.5}[PF_6]_{1.5}\cdot(MeOH)\cdot(Et_2O)\cdot(H_2O)_2$. The asymmetric unit contains 1.5 molecules of the complex, one in a general position with no imposed symmetry and the other astride a mirror plane, as well as two molecules of water, one of methanol, and one of ether. Potential problems with overlapping low-angle reflections due to the long *c* axis (43.41 Å) were minimized by using a narrow detector aperture.

$[M(Tp^{Py})(NO_3)_2]$ (M = Pr, Eu, Er) all crystallize with some solvent molecules that are severely disordered about inversion centers and could not be accurately modeled, even with data collection at 173 K. In each case, the collection of electron density maxima was modeled with carbon atoms using fractional site occupancies. For M = Pr, the solvents may be approximated as two molecules of ether: 12 sites were refined as carbon atoms with fractional site occupancies adding up to

Table 5. Selected Bond Lengths (Å) and Angles (deg) for $[M(Tp^{Py})_2][BPh_4]$ (M = Sm, Eu)

	Sm	Eu		Sm	Eu
M(1)−N(121)	2.661(5)	2.643(3)	M(2)−N(221)	2.636(5)	2.643(3)
M(1)−N(141)	2.652(5)	2.677(3)	M(2)−N(241)	2.651(6)	2.670(3)
M(1)−N(161)	2.667(6)	2.661(3)	M(2)−N(261)	2.678(5)	2.631(3)
M(1)−N(111)	2.935(6)	2.920(3)	M(2)−N(211)	2.913(6)	2.967(3)
M(1)−N(131)	2.929(6)	2.971(3)	M(2)−N(231)	2.976(6)	2.970(3)
M(1)−N(151)	2.972(6)	2.947(3)	M(2)−N(251)	2.973(6)	2.897(3)

N(121)−Sm(1)−N(141)	68.1(2)	N(121a)−Eu(1)−N(141)	68.18(10)
N(121)−Sm(1)−N(161)	68.5(2)	N(121a)−Eu(1)−N(161)	68.06(10)
N(141)−Sm(1)−N(161)	68.5(2)	N(141)−Eu(1)−N(161)	68.42(10)
N(111)−Sm(1)−N(121)	57.9(2)	N(111)−Eu(1)−N(121)	58.77(10)
N(131)−Sm(1)−N(141)	58.4(2)	N(131)−Eu(1)−N(141)	57.92(10)
N(151)−Sm(1)−N(161)	57.9(2)	N(151)−Eu(1)−N(161a)	58.23(10)
N(111)−Sm(1)−N(131a)	62.3(2)	N(111)−Eu(1)−N(131)	61.82(9)
N(131a)−Sm(1)−N(151)	61.8(2)	N(131)−Eu(1)−N(151)	62.76(9)
N(151)−Sm(1)−N(111a)	62.4(2)	N(151)−Eu(1)−N(111a)	62.11(9)
N(125)−B(1)−N(165)	109.2(7)	N(125)−B(1)−N(165a)	109.5(4)
N(125)−B(1)−N(145)	110.1(6)	N(125)−B(1)−N(145a)	109.6(4)
N(145)−B(1)−N(165)	109.8(6)	N(145a)−B(1)−N(165a)	109.5(4)
N(221)−Eu(2)−N(241)	67.6(2)	N(221a)−Eu(2)−N(241)	69.35(10)
N(221)−Eu(2)−N(261)	68.0(2)	N(221a)−Eu(2)−N(261)	67.65(10)
N(241)−Eu(2)−N(261)	69.2(2)	N(241)−Eu(2)−N(261)	68.05(10)
N(211)−Eu(2)−N(221)	59.0(2)	N(211)−Eu(2)−N(221)	58.45(10)
N(231)−Eu(2)−N(241)	58.2(2)	N(231)−Eu(2)−N(241)	57.89(10)
N(251)−Eu(2)−N(261)	57.6(2)	N(251)−Eu(2)−N(261)	59.20(10)
N(211)−Eu(2)−N(231a)	62.2(2)	N(211)−Eu(2)−N(231)	61.79(9)
N(231a)−Eu(2)−N(251)	61.5(2)	N(231)−Eu(2)−N(251a)	62.95(9)
N(251)−Eu(2)−N(211a)	63.0(2)	N(251)−Eu(2)−N(211)	62.38(9)
N(225)−B(2)−N(265)	109.8(6)	N(225)−B(2)−N(265a)	109.6(3)
N(225)−B(2)−N(245)	110.1(6)	N(225)−B(2)−N(245a)	109.4(4)
N(245)−B(2)−N(265)	109.6(6)	N(245a)−B(2)−N(265a)	109.0(4)

(19) (a) SHELXTL 5.03 program system; Siemens Analytical X-Ray Instruments, Madison, WI, 1995. (b) Software package for use with the SMART diffractometer; Siemens Analytical X-Ray Instruments, Madison, WI, 1995.

a total of 10 atoms. For M = Eu and Er, the disordered solvents could be approximated as one molecule of dmf in a general position and half a molecule of ether on an inversion center, which comprised four atoms (all modeled as carbon) whose fractional site occupancies added up to 2.5. The solvent atoms were allowed to refine anisotropically but with isotropic restraints applied; no hydrogen atoms were included.

$[Sm(Tp^{py})_2][BPh_4]\cdot(Et_2O)$ and $[Eu(Tp^{py})_2][BPh_4]\cdot(Et_2O)$ are likewise very similar. In each case the asymmetric unit contains two independent half-molecules astride inversion centers and one ether molecule.

Selected bond lengths and angles for the crystal structures are collected in Tables 3−5.

Results and Discussion

Synthesis of the Ligand. Synthesis of Tp^{Py} (as its potassium salt) follows the usual route for the preparation of substituted tris(pyrazolyl)borates,[7] from reaction of 3-(2-pyridyl)pyrazole with KBH_4 in a melt. Good yields were obtained even when a considerable excess of 3-(2-pyridyl)pyrazole was used. Further reaction to give the tetrakis(pyrazolyl)borate did not occur, and use of excess of the pyrazole ensured that contamination of the product with bis[3-(2-pyridyl)pyrazolyl]dihydroborate did not occur; this was a significant byproduct when only a stoichiometric amount of 3-(2-pyridyl)pyrazole was used.

Molecular modeling studies (using a CAChe workstation and the proprietary software)[20] indicated that the cavity of Tp^{Py} would be of an appropriate size for lanthanide(III) ions. We reacted KTp^{Py} with a variety of lanthanide salts in different stoichiometries and found that two types of complex form, depending on the conditions.

Synthesis and Characterization of 1:1 Complexes with Lanthanides. Reaction of KTp^{Py} with lanthanide salts in a 1:1 ratio in methanol as solvent, in the presence of other species that can also coordinate to lanthanides, give complexes of the type $[M(Tp^{Py})L_n]^{m+}$ in which the lanthanide is coordinated by one hexadentate podand ligand, and the remaining coordination sites are occupied by whatever appropriate small ligands (counterions, solvent molecules) were present in the reaction medium. Thus, reaction of equimolar amounts of MCl_3 (M = Sm, Eu, Gd, Tb, Ho, Yb) and KTp^{Py} in MeOH followed by precipitation of the complex cation by addition of NH_4PF_6 to the solution afforded rather unexpectedly the complexes $[M(Tp^{Py})(MeOH)_2F][PF_6]$ (**A**), in which the strongly coordinated fluoride ion originated from a hexafluorophosphate ion, and two solvent molecules complete the nine-coordinate structure. FAB mass spectra of these complexes showed in every case a molecular ion $\{M(Tp^{Py})F\}^+$ in which the fluoride ion is retained. It was therefore not apparent from the mass spectra what the remaining ligands were, and elemental analyses unfortunately proved unreliable for this series of complexes, with repeated analyses on the same batch of crystalline material giving very variable results with rather low % C and % N figures. Addition of combustion aids and use of extreme combustion conditions did not improve matters. This has been a general feature of many of lanthanide complexes described in this paper, particularly series **A** and **C**.

To determine the formulations of the **A** complexes we therefore resorted to crystallographic analysis. The X-ray structure of $[Eu(Tp^{Py})(MeOH)_2F][PF_6]$ is in Figure 1 (see Table 3). The Eu(III) is nine-coordinated by the six donor atoms of Tp^{Py}, two methanol ligands, and the fluoride ion. The unit cell contains two independent complex units, one in a general position and one astride a mirror plane; only the former is depicted in Figure 1 and used as a basis for the discussion of the structure, but the bond lengths and angles of the complex unit on the mirror plane are similar. The bonds to the three pyrazolyl nitrogens at the "top" of the cavity (average length

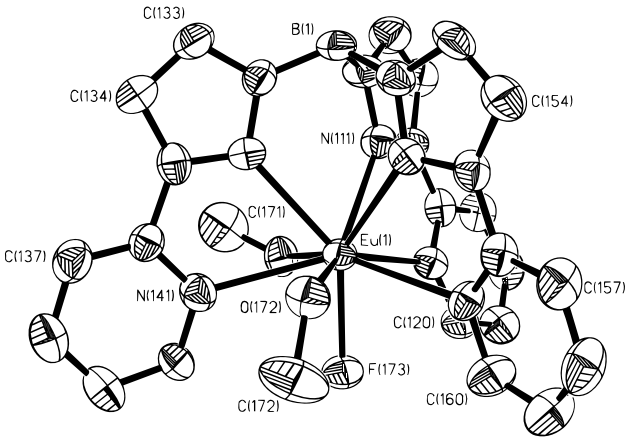

Figure 1. Structure of one of the independent complex cations of $[Eu(Tp^{Py})F(MeOH)_2][PF_6]$.

2.54 Å) are significantly shorter than those to the pyridyl nitrogen atoms at the "bottom" of the cavity (average length 2.67 Å), which seems to be due to the steric limitations of the ligand−since the three coordinating arms are diverging, closer coordination of the pyridyl donors would impose steric strain on the ligand. The bite angles of the chelating arms are all ∼62°. The ligand is considerably distorted away from C_3 symmetry, particularly in the disposition of the pyridyl rings: whereas the three apical N−B−N angles are fairly similar, the separation between N(121) and N(161) is much less than those between N(121)−N(141) and N(141)−N(161). This allows methanol ligands to attach to the metal in the spaces between N(121) and N(141) and between N(161) and N(141): in fact N(121), N(161), O(172), N(141), and O(171) very roughly describe a pentagonal plane. The coordination geometry of the Eu(III) is monocapped square antiprismatic, with N(111), N(151), N(121), and N(161) forming one square plane; N(131), the two oxygen donors and the fluoride ion the next square plane; and N(141) being the cap. On the basis of the similarity of their IR spectra, we assume that the rest of the **A** complexes have the same $[M(Tp^{Py})F(MeOH)][PF_6]$ formulation.

Seeking to prepare similar 1:1 complexes in a more controlled and predictable manner, lanthanide nitrate salts were used instead and afforded a range of complexes $[M(Tp^{Py})(NO_3)_2]$ (series **B**; M = La, Pr, Sm, Eu, Gd, Tb, Er) in which those coordination sites on the metal not occupied by Tp^{Py} are blocked by nitrate ligands. The constitution of these complexes is therefore not solvent dependent. These 1:1 complexes were characterized on the basis of their FAB mass spectra, IR spectra, and (in some cases) elemental analyses. The FAB spectra generally showed a strong peak corresponding to $\{M(Tp^{Py})(NO_3)\}^+$ arising from loss of one coordinated nitrate. Elemental analytical data for the **B** complexes were much better than for the **A**, and accurate analyses consistent with the formulation $[M(Tp^{Py})(NO_3)_2]$ were obtained for about half of the series: the remaining complexes behaved like the **A** complexes, with erratic and low % C and % N values even on vacuum-dried samples from hand-picked X-ray quality single crystals.

The IR spectra are very similar across the series and show only one B−H stretching vibration. Comparison of the IR spectra with the **A** complexes revealed the presence of three strong bands at ∼1460, 1385, and 1310 cm^{-1} in each case, of which some or all must be due to the coordinated nitrate ligands. Determination of the mode of coordination of nitrate ions from IR data is not straightforward,[21] but the bands at ∼1460 and 1310 cm^{-1} could be the ν_1 and ν_4 modes of a bidentate nitrate.[11a]

Confirmation of the formulation was again provided crystallographically. The structures of $[M(Tp^{Py})(NO_3)_2]$ (M = Er,

(20) CAChe Scientific, Beaverton, OR, 1994.

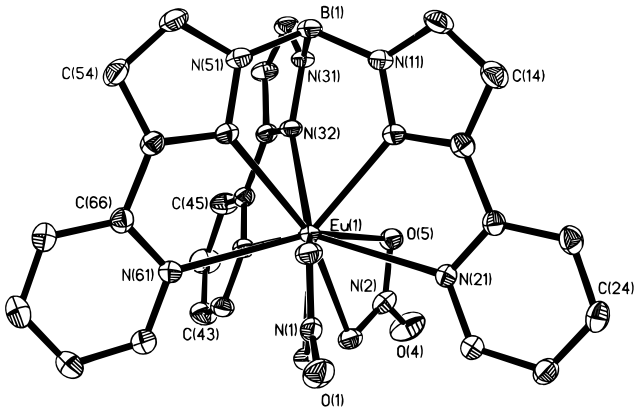

Figure 2. Structure of the complex $[Eu(Tp^{Py})(NO_3)_2]$.

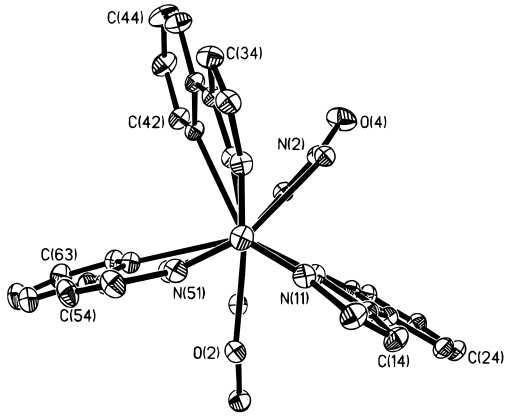

Figure 3. View of $[Eu(Tp^{Py})(NO_3)_2]$, along the Eu−B axis, emphasizing the asymmetric coordination mode of Tp^{Py} and the positions of the nitrate ligands.

Eu, Pr) are all very similar and accordingly only that of the europium(III) complex is shown in Figures 2 and 3 (see Table 4). The complexes are 10-coordinate, with a hexadentate Tp^{Py} podand and two bidentate nitrates. The differences in the two M−O bond lengths for each coordinated nitrate group are small so the nitrates may be considered to be coordinated in a symmetric bidentate manner. The general disposition of the Tp^{Py} ligand is similar to that observed in $[Eu(Tp^{Py})(MeOH)_2F][PF_6]$, with two of the arms lying close to one another to create gaps to accommodate the nitrate ligands (Figure 3). One apical N−B−N angle is correspondingly smaller than the other two [105−107° for N(31)−B−N(51) in each case, compared to 109.2−110.8° for the other apical N−B−N angles]. There is a clear correlation between the M−N bond lengths and the ionic radii of the metals. From Pr(III) to Er(III) a decrease in ionic radius of ∼0.1 Å is expected. Between the Pr(III) and Er(III) complexes, the average metal−N(pyridyl) distance decreases from 2.73 to 2.66 Å, a drop of 0.07 Å, and the average metal−N(pyrazolyl) distance decreases from 2.57 to 2.46 Å, a drop of 0.09 Å. The bite angles of the chelating arms increase as the metal size decreases, with average bite angles of 61.0, 62.2, and 62.8° for M = Pr, Eu, and Er, respectively. The flexibility of the ligand is evidently enough to allow the cavity size to change within reasonable limits to accommodate the different sizes of the lanthanide ions.

Within the unit cell of these complexes, two molecules are related by an inversion center (Figure 4). The packing arrangement is such that there is graphitic π-stacking between the near-planar bidentate arms of adjacent molecules, with the separation between the overlapping planes lying in the range 3.3−3.6 Å. In addition the noncoordinated oxygen atom of one of the nitrate groups is involved in a weak hydrogen-bonding interaction to a peripheral CH proton on the adjacent molecule (O···H separations are all ∼2.5 Å).

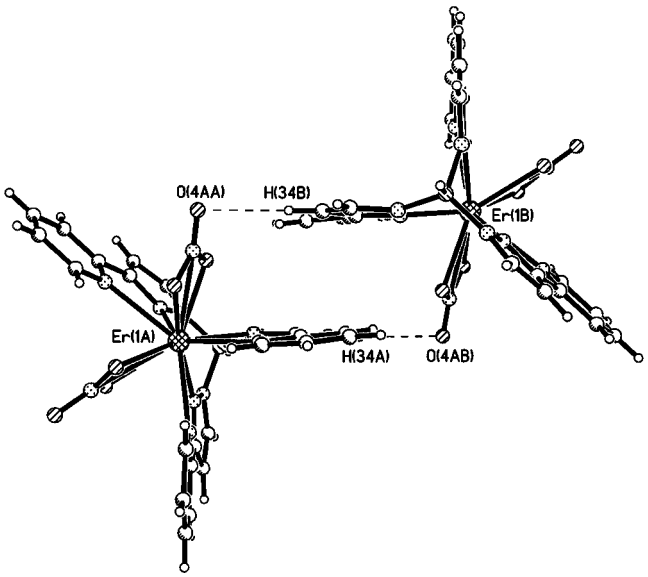

Figure 4. View of $[Er(Tp^{Py})(NO_3)_2]$ showing the intermolecular hydrogen bonding and π-stacking across the inversion center.

Synthesis and Characterization of 1:2 Complexes with Lanthanides. In order to see what types of complex would form in the absence of any strongly coordinating anions, we reacted KTp^{Py} with various MCl_3 salts in methanol and used $[BPh_4]^-$ as the anion. In this way the coordination of fluoride or nitrate ions, which plays an important role in determining the structures of the 1:1 complexes, could be avoided. The resulting complexes are of the form $[M(Tp^{Py})_2][BPh_4]$ (series **C**; M = La, Sm, Eu, Gd, Tb), and their yields were subsequently optimized by use of a 1:2 metal:ligand ratio. Again, characterization was on the basis of FAB mass spectra, limited elemental analyses, and IR spectra. The FAB mass spectra all showed strong peaks corresponding to $\{M(Tp^{Py})_2\}^+$, and the two reliable elemental anayses that could be obtained were consistent with the formulation $[M(Tp^{Py})_2][BPh_4]$. The IR spectra showed in every case two B−H stretching vibrations at ∼2450 and ∼2480 cm^{-1}, which could arise from coupling of the two B−H vibrations, although it is also possible that these could arise from two inequivalent sites in the crystal (below). It appears that, in the absence of coordinating anions, 2 equiv of Tp^{Py} are able to coordinate to the lanthanide ions, whereas the presence of fluoride or nitrate ions in the 1:1 complexes blocks the coordination of a second equivalent of Tp^{Py}.

The crystal structures of $[Sm(Tp^{Py})_2][BPh_4]$ and $[Eu(Tp^{Py})_2][BPh_4]$ were both determined and are essentially identical; Figures 5 and 6 depict the Eu(III) complex (see Table 5). In both cases the unit cell contains two crystallographically independent molecules which both lie on inversion centers (i.e., the asymmetric unit contains two independent half-molecules). There are no substantial differences between the independent complex cations in each structure.

The two ligands neatly interpenetrate to give 12-coordination of the metal centers, with an approximately icosahedral (3:6:3′) coordination geometry (3 and 3′ denote mutually staggered sets of pyrazolyl donor atoms, and the 6 denotes the puckered arrangement of six pyridyl donor atoms interleaved around the

(21) (a) Addison, C. C.; Logan, N.; Wallwork, S. C.; Garner, C. D. *Q. Rev.* **1971**, *25*, 289. (b) Ferraro, J. R.; Cristallini, C.; Fox, I. *J. Inorg. Nucl. Chem.* **1967**, *29*, 139. (c) Nakamoto, K. *Infra-red and Raman Spectra of Inorganic and Coordination Compounds*, 3rd ed.; Wiley: New York, 1978.

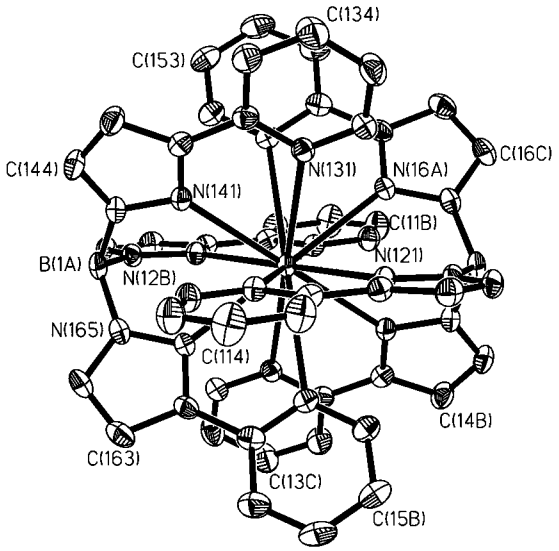

Figure 5. Structure of one of the independent cations of $[Eu(Tp^{Py})_2][BPh_4]$.

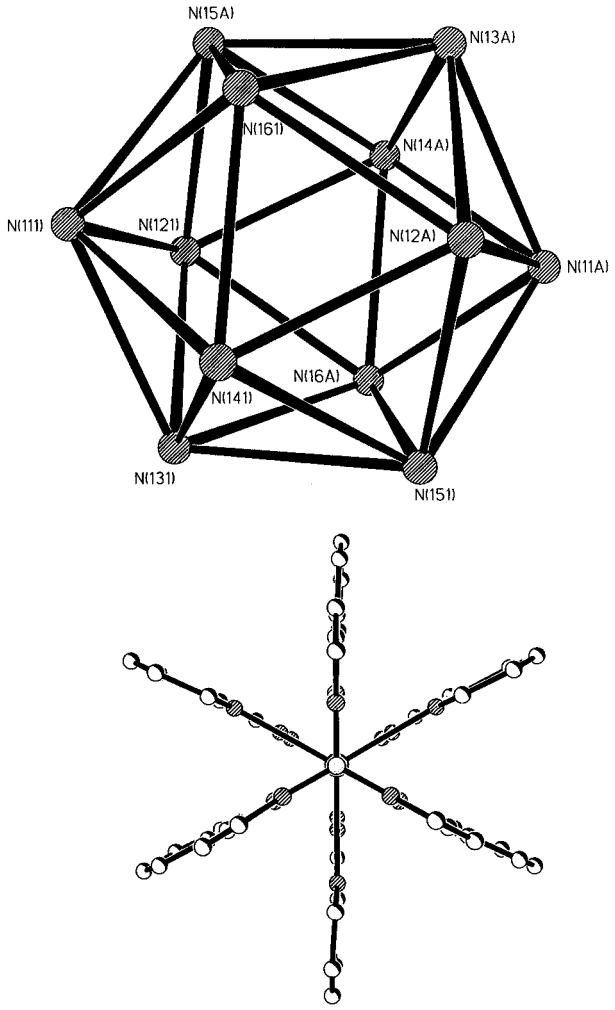

Figure 6. (a, top) Near-icosahedral coordination geometry of the $[Eu(Tp^{Py})_2]^+$ cation [the Sm(III) analogue is essentially identical]; (b, bottom) a view along the B−Eu−B axis showing the interpenetration of the ligands and the pseudo-C_3 symmetry.

equator).[22] The main distortion from ideal icosahedral geometry is a compression along the B−M−B axis, such that the dihedral angles between the faces either side of the six pyridyl−pyridyl edges are ∼130° instead of the ideal 138°, whereas the dihedral angles between the faces either side of the pyrazolyl−pyrazolyl edges are ∼142°. Consequently the metal−pyridyl bonds (average length 2.95 Å) are ∼0.29 Å longer than the metal−pyrazolyl bonds (average length 2.66 Å). This is a steric consequence of having six pyridyl ligands around the equator of the complex; in $[Eu(Tp^{py})F(MeOH)_2][PF_6]$, for example, the average Eu−pyridyl distance is only 0.13 Å more than the average Eu−pyrazolyl distance. As a result of the long M−N(pyridyl) distances, the bite angles of the N,N′-chelating fragments are significantly smaller than in the **A** and **B** complexes, all lying between 57 and 59°. The opposed 3 and 3′ planes of the icosahedral coordination sphere (from the pyrazolyl ligands) are exactly parallel, which is necessitated in each case by the inversion symmetry of the complexes. The apical N−B−N bonds of the ligands are 109−110°, indicating that the ligand is not having to strain to accommodate the metal ions. Figure 6 emphasises the coordination geometry, and the pseudo-C_3 symmetry about the B−M−B axis axis. Takats and co-workers recently showed that the uranium(III) complex $[U(Tp^{Py})_2]I$ also has the same icosahedral structure.[10b]

Although 12-coordination is well-known in lanthanide(III) complexes, it is largely confined to complexes containing bidentate oxyanion ligands such as nitrates in which the two donor atoms are very close together: $[La(18\text{-crown-}6)(NO_3)_3]$ and $[Nd(18\text{-ane-}N_6)(NO_3)_3]$ are typical examples.[23] The only other 12-coordinate lanthanide complexes with solely N-donor ligands are $[M(napy)_6][ClO_4]_3$ (napy = 1,8-naphthyridine;[24] M = La, Ce, Pr) and $[La(ctthb)_4][ClO_4]_3$ (ctthb = *cis*-triazatris-σ-homobenzene),[25] in both of which the high coordination number was ascribed to the unusual proximity of the N-donor atoms within each ligand. With more conventional ligands such as polypyridines, coordination numbers of 8 or 9 are usual.[26]

Solution Conductivity Studies. The conductivities of the **B** complexes were measured in CH_2Cl_2 and water. In water, the molar conductivites of the series **B** complexes all lie in the region 200−250 Ω^{-1} cm^2 mol^{-1}. The ionic conductivity of the nitrate ion in water is 71.5 Ω^{-1} cm^2 mol^{-1}. Dissociation of both nitrate ions therefore results in a contribution of ∼140 Ω^{-1} cm^2 mol^{-1} to the conductivity of the complexes leaving 60−110 Ω^{-1} cm^2 mol^{-1} to be accounted for. This is a sensible value for a large dication: the value for Ba^{2+} for example is 127 Ω^{-1} cm^2 mol^{-1}, and we would expect $[M(Tp^{Py})(H_2O)_q]^{2+}$ to be rather less mobile. In contrast, if we assume dissociation of only one nitrate ion, this leaves a contribution for the monocation $[M(Tp^{Py})(NO_3)(H_2O)_q]^+$ of 130−180 Ω^{-1} cm^2 mol^{-1}, which is far too large: Cs^+ and $[Me_4N]^+$, for example, have conductivities in water of 77 and 45 Ω^{-1} cm^2 mol^{-1} respectively. The **B** complexes are therefore 1:2 electrolytes in water, forming $[M(Tp^{Py})(H_2O)_q][NO_3]_2$ in which the two nitrate ligands

(22) (a) Favas, M. C.; Kepert, D. L. *Prog. Inorg. Chem.* **1981**, *28*, 309. (b) Kepert, D. L. *Inorganic Stereochemistry;* Springer-Verlag: Berlin, 1982.

(23) (a) Backer-Dirks, J. D. J.; Cooke, J. E.; Galas, A. M. R.; Ghotra, J. S.; Gray, C. J.; Hart, F. A.; Hursthouse, M. B. *J. Chem. Soc., Dalton Trans.* **1980**, 2191. (b) Bünzli, J.-C. G.; Klein, B.; Wessner, D. *Inorg. Chim. Acta* **1980**, *44*, L147.

(24) (a) Foster, R. J.; Bodner, R. L.; Hendricker, D. G.; *J. Inorg. Nucl. Chem.* **1972**, *34*, 3795. (b) Clearfield, A.; Gopal, R.; Olsen, R. W. *Inorg. Chem.* **1977**, *16*, 911.

(25) Schwesinger, R.; Piontek, K.; Littke, W.; Prinzbach, H. *Angew. Chem., Int. Ed. Engl.* **1985**, *24*, 318.

(26) (a) Bernardinelli, G.; Piguet, C.; Williams, A. F. *Angew. Chem., Int. Ed. Engl.* **1992**, *31*, 1622. (b) Piguet, C.; Bünzli, J.-C. G.; Bernardinelli, G.; Hopfgartner, G.; Williams, A. F. *J. Am. Chem. Soc.* **1993**, *115*, 8197. (c) Frost, G. H.; Hart, F. A.; Heath, C. A.; Hursthouse, M. B. *J. Chem. Soc., Chem. Commun.* **1969**, 1421. (d) Stösser, R.; Schneider, M.; Janietz, P.; Landsberg, R. *Z. Phys. Chem. (Leipzig)* **1980**, *261*, 346. (e) Yang, C.; Chen, X.-M.; Zhang, W.-H.; Chen, J.; Yang, Y.-S.; Gong, M.-L. *J. Chem. Soc., Dalton Trans.* **1996**, 1767.

are replaced by *q* water molecules. It is unlikely that two nitrate ligands would be replaced by four water molecules for steric reasons. As mentioned earlier, nitrate-based lanthanide complexes have high coordination numbers only because the donor atoms of a bidentate nitrate are much closer together than two independent monodentate ligands could be. It is more likely that a coordination number of 9 is adopted, with three water molecules replacing the two nitrates; this is also consistent with the values of *q* determined from luminescence studies (see later).

In CH_2Cl_2 the molar conductivities of the **B** complexes were ~1000 times smaller than in water, i.e., effectively zero, and in this noncoordinating solvent, the complexes remain intact and therefore neutral.

Solution NMR Studies. In order to assist in the study of the solution properties of these complexes, we prepared the diamagnetic lanthanum(III) complexes $[La(Tp^{Py})(NO_3)_2]$ (**B**) and $[La(Tp^{Py})_2][BPh_4]$ (**C**). The spectrum of $[La(Tp^{Py})(NO_3)_2]$ in acetone-d_6 (see Experimental Section) shows the presence of six signals in the aromatic region corresponding to the four pyridyl and two pyrazolyl protons. It follows that in solution the complex has threefold symmetry with all chelating arms equivalent (C_{3v}), and the asymmetry observed in the crystal structures of the **B** complexes is only a solid-state phenomenon. There are two ways in which this could happen: a rapid fluxional rearrangement of the nitrate ligands and the Tp^{Py} ligand such that on the NMR time scale an average structure is seen or formation of a more symmetric structure by replacement of coordinated nitrates by solvent molecules. The ^1H NMR spectrum of $[La(Tp^{Py})_2][BPh_4]$ is also indicative of a symmetric C_{3v} structure, which is to be expected on the basis of the crystal structures of the Eu(III) and Sm(III) analogues. We attempted to obtain spectra of the paramagnetic **B** and **C** complexes, but in most cases the spectra were broadened to the extent where individual peaks could not be resolved.

From the solution conductivity results, it is apparent that the Gd(III) **B** complex $[Gd(Tp^{Py})(NO_3)_2]$ has all of the structural features necessary to be an effective NMR relaxation agent in water and, therefore, to be a possible prototype of a new MRI contrast agent, since dissociation of the nitrate ligands allows direct access of (rapidly exchanging) water ligands to the Gd(III) coordination sphere.[3] Accordingly we measured the T_1 relaxivity (r_1) of the **B** complexes in water: the values are 0.037 (Sm), 0.072 (Eu), 4.4 (Gd), 0.19 (Tb) and 0.17 (Er) s^{-1} mM^{-1}. The value of 4.4 s^{-1} mM^{-1} for $[Gd(Tp^{Py})(NO_3)_2]$ is comparable with many other Gd(III) complexes of polyamino carboxylate ligands that are of clinical value but that generally have *q* values of 1 or 2.[3,5b] The relaxivity of $[Gd(Tp^{Py})(NO_3)_2]$ is therefore rather less than might be expected on the basis of probably three exchanging water ligands. The relaxivity, however, depends not only on the number of exchanging water molecules but on their rate of exchange, and a slow exchange rate—which may arise through subtle steric factors—would reduce the relaxivity and may be a significant effect in $[Gd(Tp^{Py})(NO_3)_2]$.[4a] $[Gd(Tp^{Py})(NO_3)_2]$ is not itself likely to be clinically useful due to the susceptibility of the tris(pyrazolyl)borate fragment to decomposition by acid hydrolysis, but this problem could be circumvented (e.g., by steric protection of the boron atom) and we are currently investigating this.

Luminescence Studies on $[M(Tp^{Py})(NO_3)_2]$ (M = Eu, Tb). All of the complexes have two intense transitions in the UV region of the electronic spectrum arising from ligand-based $\pi-\pi^*$ transitions. The wavelengths of these transitions are virtually constant across the entire series, being 288 ± 3 and 242 ± 3 nm, with extinction coefficients in the range $(1-4) \times 10^4$ and the 242 nm transition always being ~50% more intense than the 288 nm transition. In the Eu(III) and Tb(III) complexes, which have luminescent f−f excited states that cannot effectively be excited by direct absorption of light, excitation of the ligand-based $\pi-\pi^*$ transitions is followed by metal-centerd luminescence due to efficient energy transfer from the ligand-based excited state to the metal-based excited state. This type of sensitisation is well-known in lanthanide complexes containing aromatic ligands.[2]

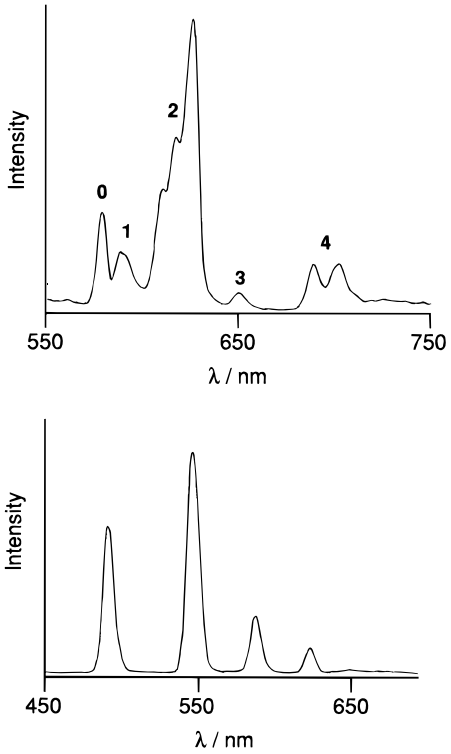

Figure 7. Emission spectra in fluid solution at 295 K of $[Eu(Tp^{Py})(NO_3)_2]$ in MeOH (top) and $[Tb(Tp^{Py})(NO_3)_2]$ in CH_2Cl_2 (bottom). The labels 0−4 on the upper spectrum refer to the $^5D_0 \rightarrow {}^7F_n$ ($n = 0-4$, respectively) transitions.

For the **B** complexes $[Eu(Tp^{Py})(NO_3)_2]$ and $[Tb(Tp^{Py})(NO_3)_2]$, representative spectra (room temperature, fluid solution) are shown in Figure 7 following excitation at the maximum of the ligand-based $\pi-\pi^*$ transitions. The spectrum of $[Eu(Tp^{Py})(NO_3)_2]$ in methanol shows the expected series of $^5D_0 \rightarrow {}^7F_n$ ($n = 0-4$) transitions. The spectrum of $[Tb(Tp^{Py})(NO_3)_2]$ is stronger and better resolved and shows the expected sequence of $^5D_4 \rightarrow {}^7F_n$ transitions, with the $n = 6$, 5, 4, and 3 components being visible. No further splitting of these was visible, and the spectrum is entirely typical. Because of the relatively poor resolution of the (weak) spectrum of $[Eu(Tp^{Py})(NO_3)_2]$, it is not possible to determine whether or not the $^5D_0 \rightarrow {}^7F_0$ transition is split, which would indicate the number of Eu(III) environments in solution.[17,27] The intensity of the $^5D_0 \rightarrow {}^7F_0$ transition is significant, however; although it is formally forbidden it can gain intensity by "*J* mixing" in certain ligand fields[28] and can become quite strong in, *inter alia*, C_{3v} symmetry (but not C_{3h} or D_{3h}), which is consistent with the symmetric NMR spectrum observed for the La(III) analogue. Likewise the appearance of three components for the hypersensitive $^5D_0 \rightarrow {}^7F_2$ transition is consistent with C_{3v} symmetry in solution since a fivefold-degenerate $J = 2$ state would split to give one A_1 and two E sublevels. The spectra of both complexes remained unchanged in water and methanol over several hours, indicating that the tris(pyrazolyl)borate ligand does not solvolyze at neutral pH.

(27) Bryden, C. C.; Reilley, C. N. *Anal. Chem.* **1982**, *54*, 610.
(28) Peacock, R. D. *Struct. Bonding (Berlin)* **1975**, *22*, 83.

Table 6. Luminescence Lifetime Data and Derived Solvation Values for Eu(III) and Tb(III) Complexes

	τ,[a] ms					q[b]	
	CH_2Cl_2	MeOH	MeOD	H_2O	D_2O	H_2O	MeOH
$[Eu(Tp^{Py})(NO_3)_2]$	1.03	0.50	1.40	0.26	1.49	3.3	2.7
$[Tb(Tp^{Py})(NO_3)_2]$	1.36	1.14	1.74	0.63	1.50	3.9	2.5
$[Tb(Tp^{Py})_2][BPh_4]$	*c*	1.26	2.08	*d*	*d*	*d*	2.6

[a] Error in lifetimes, ±0.03 ms. [b] Error in q values, ± 0.5. [c] Not determined. [d] Complex insoluble in water.

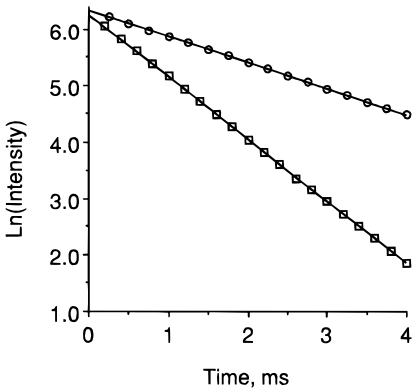

Figure 8. Emission decay profiles for $[Tb(Tp^{Py})(NO_3)_2]$ in H_2O (squares) and D_2O (circles).

However, addition of a drop of acid resulted in immediate and almost complete loss of the luminescence. A more detailed study of the luminescence spectra of these complexes (including a low-temperature study) is in progress and will be the subject of a separate report.[29]

The metal-centered emission lifetimes were determined by monitoring the decay of the $^5D_0 \rightarrow {}^7F_2$ transition (615 nm) for the Eu(III) complex, and the $^5D_4 \rightarrow {}^7F_5$ transition (550 nm) for the Tb(III) complex, and are collected in Table 6. They show that in good donor solvents such as water and methanol the lifetimes of the metal-centerd emissions are considerably shorter than in CH_2Cl_2, where replacement of nitrate by solvent does not occur and solvent-based quenching is therefore restricted to outer-sphere effects.[6b] Comparison of the luminescence lifetimes of $[Eu(Tp^{Py})(NO_3)_2]$ (M = Eu, Tb) in H_2O and D_2O allows an estimation of the value of q, the number of coordinated water ligands in the hydrated species. Similarly, measurements in MeOH and MeOD allow estimation of the number of coordinated methanol ligands.[2a,17] For both complexes the lifetimes were substantially longer in the deuterated solvents than the protonated ones, due to the well-known greater quenching efficiency of the O−H group compared to the O−D group.[17] Typical decay curves are given in Figure 8, and the values of q determined from these lifetimes are also in Table 6. The number of coordinated water molecules—3.3 for the Eu(III) complex and 3.9 for the Tb(III) complex—is in agreement with the conductivity measurements which showed that both nitrate ions dissociate, and the average q value of 3.6 (±0.5) suggests the presence of three coordinated water ligands with an additional small contribution arising from outer-sphere solvation. It has been shown by Parker and co-workers that in complexes with no water ligands *directly* coordinated to the lanthanide center, second-sphere coordination and/or hydrogen bonding of water molecules can still lead to significant lifetime differences between H_2O and D_2O, leading to apparent q values anywhere between 0 and 1.[6b] The number of coordinated methanol molecules is somewhat less, being on average 2.6 (±0.5), which may reflect the increased steric bulk of methanol ligands compared to water or incomplete dissociation of nitrate. However, given the errors associated with this crude calculation, this difference does not merit detailed discussion.

Luminescence Studies on $[M(Tp^{Py})_2][BPh_4]$ (M = Eu, Tb). The emission behavior of the 12-coordinate **C** complexes $[M(Tp^{Py})_2][BPh_4]$ (M = Eu, Tb) is less straightforward. $[Tb(Tp^{Py})_2][BPh_4]$ gave a typical emission spectrum [like that shown for $[Tb(Tp^{Py})(NO_3)_2]$ in Figure 7]. However, the spectrum of $[Eu(Tp^{Py})_2][BPh_4]$ in fluid solution was weak and poorly resolved, and the intensities of the components varied unpredictably between solvents. A more detailed study of the luminescence properties of these complexes in in progress.[29]

Lifetime measurements in MeOH and MeOD again give useful information regarding the extent of solvation of the complexes in solution. For $[Tb(Tp^{Py})_2][BPh_4]$, the substantial difference between the lifetimes in MeOH and MeOD (Table 6) gives a value for the solvation parameter q of 2.6. This is identical to the values obtained for the **B** complexes in which the nitrate ions are labile in donor solvents. It follows that although $[Tb(Tp^{Py})_2][BPh_4]$ is coordinatively saturated (12-coordinate) in the solid state, in solution detachment of one or more bidentate ligand arms occurs, which allows access of solvent molecules to the metal coordination sphere. We note (i) that in the crystal structures of the 12-coordinate Eu(III) and Sm(III) complexes the six M−N(pyridyl) bonds around the "equator" are unusually long (Table 5), and therefore presumably weak, due to steric congestion arising from interpenetration of the two ligands; and (ii) the coordination mode for $[Tp^{Py}]^-$ in which two arms are coordinated and one is pendant is known in other complexes.[11a,b] Accurate lifetime measurements for $[Eu(Tp^{Py})_2][BPh_4]$ could not be obtained as the luminescence decay was not single exponential, possibly indicating a mixture of species with different degrees of solvation. These **C** complexes are insoluble in water so we could not compare the lifetimes in D_2O and H_2O.

Conclusions

The hexadentate podand ligand $[Tp^{Py}]^-$ can react with lanthanide(III) ions to give nine- or ten-coordinate 1:1 complexes $[M(Tp^{Py})L_n]^{n+}$, or twelve-coordinate 1:2 complexes $[M(Tp^{Py})_2][BPh_4]$, depending on the presence or absence of other ligands L in the reaction mixture. Six complexes have been characterized crystallographically. The 1:1 complexes $[M(Tp^{Py})(NO_3)_2]$ dissociate in water to give $[M(Tp^{Py})(H_2O)_q](NO_3)_2$, in which q is probably 3. The Gd(III) complex of this series is effective at bulk relaxation of solvent water (relaxivity = 4.4 s^{-1} mM^{-1}) and is accordingly a prototypical MRI contrast enchancement agent. Luminescence lifetime studies on the 1:1 complexes $[M(Tp^{Py})(NO_3)_2]$ (M = Eu, Tb) confirm that dissociation of nitrates in water and methanol permits solvent-based quenching, with effective solvation numbers q of 3.6 and 2.6 for water and methanol respectively. Luminescence lifetime studies on the 12-coordinate complex $[Tb(Tp^{Py})_2][BPh_4]$ also show that solvent-based quenching can occur (q = 2.6 for methanol), which suggests that one or more bidentate ligand arms peels off the metal to allow access of the solvent molecules to the coordination sphere. The luminescence behavior of $[Eu(Tp^{Py})_2][BPh_4]$ is complex and not fully understood.

Acknowledgment. We thank the EPSRC and Unilever Research for financial support.

Supporting Information Available: Tables of X-ray experimental details and crystallographic data, all atomic coordinates, anisotropic thermal parameters, and bond distances and angles, for the six crystal structures (72 pages). Ordering information is given on any current masthead page.

IC960621M

(29) Armaroli, N.; Barigelletti, F.; Jones, P. L.; McCleverty, J. A.; Ward, M. D. unpublished results.